Adv. Sci. Res., 10, 7–13, 2013
www.adv-sci-res.net/10/7/2013/
doi:10.5194/asr-10-7-2013

Advances in Science & Research
Open Access Proceedings

Sensitivity of the RMI's MAGIC/Heliosat-2 method to relevant input data

C. Demain, M. Journée, and C. Bertrand

Royal Meteorological Institute of Belgium, Brussels, Belgium

Correspondence to: M. Journée (michel.journee@meteo.be)

Received: 27 September 2012 – Revised: 17 December 2012 – Accepted: 26 December 2012 – Published: 16 January 2013

Abstract. Appropriate information on solar resources is very important for a variety of technological areas. Based on the potential of retrieving global horizontal irradiance from satellite data, an enhanced version of the Heliosat-2 method has been implemented at the Royal Meteorological Institute of Belgium to estimate surface solar irradiance over Belgium from Meteosat Second Generation at the SEVIRI spatial and temporal resolution. In this contribution, sensitivity of our retrieval scheme to surface albedo, atmospheric aerosol and water vapor contents is investigated. Results indicate that while the use of real-time information instead of climatological values can help to reduce to some extent the RMS error between satellite-retrieved and ground-measured solar irradiance, only the correction of the satellite-derived data with in situ measurements allows to significantly reduce the overall model bias.

1 Introduction

There are several methods for converting satellite images into surface solar irradiance (SSI). The Heliosat-2 method (Rigollier et al., 2004) is a well-known method of inverse type. The principle of the method is that a difference in global radiation perceived by the sensor aboard a satellite is only due to a change in the apparent albedo, which is itself due to an increase of the radiation emitted by the atmosphere towards the sensor (i.e., Cano et al., 1986; Raschke et al., 1987). A key parameter is the cloud index (also denoted as effective cloud albedo), n, determined by the magnitude of change between what is observed by the sensor and what should be observed under a very clear sky. To evaluate the all-sky SSI, a clear-sky model is coupled with the retrieved cloud index which acts as a proxy for cloud transmittance. Inputs to the Heliosat-2 method are not the visible satellite images in digital counts as in the original version of the method (Cano et al., 1986) but images of radiances/reflectances:

$$n^t(i,j) = \frac{\rho^t(i,j) - \rho^t_{cs}(i,j)}{\rho^t_{max}(i,j) - \rho^t_{cs}(i,j)} \quad (1)$$

where $n^t(i,j)$ is the cloud index at time t for the pixel (i,j); $\rho^t(i,j)$ is the reflectance or apparent albedo observed by the sensor at time t; $\rho^t_{max}(i,j)$ is the apparent albedo of the brightest cloud at time t; $\rho^t_{cs}(i,j)$ is the apparent ground albedo under clear-sky condition at time t. With calibrated radiances as input, Heliosat-2 offers the opportunity to replace some of the empirical parameters in the scheme with known physical quantities from external sources.

A modified version of the Heliosat-2 calculation scheme has been implemented at the Royal Meteorological Institute of Belgium (RMI) to retrieve SSI values from Meteosat Second Generation (MSG; Schmetz et al., 2002) satellite over Belgium. Section 2 presents the modifications/adaptations made to the method at RMI to exploit the enhanced capabilities of MSG in the SSI retrieval. Performance of our algorithm is discussed in Sect. 3. Sensitivity of the retrieval scheme to clear-sky model input data is presented in Sect. 4. Final remarks and conclusion are given in Sect. 5.

2 Description of the MAGIC/Heliosat-2 method implemented at RMI

The method takes advantage of the enhanced capabilities of the Spinning Enhanced Visible and Infrared Imager (SEVIRI) on board of the MSG platform through an improved scene identification and applies the Modified Lambert Beer function (Müller et al., 2004) within an eigen-vector hybrid

look-up table (LUT) approach (Müller et al., 2009) for the clear-sky irradiance computation. It is based on the LibRadTran (Mayer and Kylling, 2005) radiative transfer model (RTM) and enables the use of extended information about the atmospheric state. The source code of the clear-sky model (Mesoscale Atmospheric Global Irradiance Code – MAGIC) is available under gnu-public license at http://sourceforge.net/projects/gnu-magic/. It is worth pointing out that even if the SEVIRI sensor comprises a high spatial resolution broadband visible channel (HRV, High Resolution Visible) and that the Heliosat method was originally conceived for working with broadband images, the algorithm as in Posselt et al. (2011) is applied to the visible narrow-band channels of SEVIRI (centered at 0.6 μm (VIS06) and 0.8 μm (VIS08), respectively). Indeed, while the MSG HRV channel has a higher spatial sampling distance than the SEVIRI spectral channels (i.e., 1 km vs. 3 km at the subsatellite point, respectively), Journée et al. (2012) have shown that for a mid-latitude region with a rather flat orography like Belgium, the MSG-based daily SSI retrieval is much more sensible to the temporal resolution than to the spatial resolution of the satellite images. Therefore, only working with SEVIRI spectral images does not require to deal with the georeferencing of the MSG HRV images (e.g., the original HRV geolocation performed by the EUMETSAT ground segment is only accurate up to ±3 HRV pixels) which allows to save CPU time without a noticeable loss of precision. The retrieval process runs over a spatial domain ranging from 48.0° N to 54.0° N and from 2.0° E to 7.5° E within the MSG field-of-view. In this domain, the SEVIRI spatial sampling distance degrades to about 6 km in the north–south direction and 3.3 km in the east–west direction.

The schematic view of the procedure is shown in Fig. 1. First, cloud mask, snow mask and cloud phase are derived over the domain in real time for each 15-min MSG time slot with the EUMETSAT Satellite Application Facility on Support to Nowcasting and Very Short Range Forecasting (NWC SAF) software (Derrien and Le Gléau, 2005) using the MSG SEVIRI spectral information and 24 h numerical weather forecasts from the European Centre for Medium-Range Weather Forecasts (ECMWF) two times a day. In parallel, the SEVIRI VIS06 and VIS08 data are converted from counts to reflectance.

Second, at the end of each day, the VIS06 and VIS08 reflectances and the NWC SAF algorithm products related to the 96 MSG time slots of the elapsed day are used to determine the effective cloud albedo (or cloud index), n. For each pixel in the image and each daytime MSG time slot, clear-sky reflectances in the VIS06 and VIS08 spectral bands, ρ_{clr}, are determined from a trailing window of 60 days MSG SEVIRI reflectances at 0.6 μm and 0.8 μm, respectively, according to Ipe et al. (2003). Overcast visible reflectances, ρ_{max}, at 0.6 and 0.8 μm are determined by a LUT approach using the cloud phase information provided by the NWC SAF software. It relies on the LibRadTran (Mayer and Kylling, 2005) simulated outgoing radiances in the SEVIRI 0.6 and 0.8 μm spectral bands. RTM computations were performed assuming a cloud optical depth of 128 and a pure cloud thermodynamic phase (i.e., water cloud or ice cloud). Because of the low reflectance of a majority of natural land surfaces at 0.6 μm and the reduced influence of the vegetation seasonal cycle on the reflectance signature at this wavelength (Asner, 1998), the algorithm is applied to the VIS06 channel over land surface and to the VIS08 channel over water surface. Based on the NWC SAF cloud and snow masks the computed cloud index at 0.6 and 0.8 μm are either corrected or not corrected for possible cloud shadow or snow contamination.

Third, SSI is derived for each pixel and MSG time slot by the combination of the satellite clearness index $k(n)$ (a decreasing function of n, Hammer et al., 2003) and $\mathrm{SSI_{clr}}$, the corresponding clear-sky surface irradiance calculated by MAGIC:

$$\mathrm{SSI} = k(n) \cdot \mathrm{SSI_{clr}} \tag{2}$$

Note that for effective cloud albedo values between 0 and 0.8, SSI is the clear-sky irradiance which is not reflected back to space by clouds:

$$\mathrm{SSI} = (1 - n) \cdot \mathrm{SSI_{clr}} \tag{3}$$

Finally, the MSG retrieved all-sky SSI are integrated over the entire diurnal cycle and merged with the corresponding daily global solar irradiation recorded within the Belgian ground radiometric network operated by RMI.

3 Performance of the RMI MAGIC/Heliosat-2 retrieval scheme

The key factor determining the short-term variability of the all-sky irradiance is cloudiness. While the Heliosat-2 method is normally capable of reproducing most of the irradiance variability caused by clouds (i.e., Hammer et al., 2003; Rigollier et al., 2004; Lefèvre et al., 2007; Moradi et al., 2009), current satellite instruments are insufficient to accurately sense small broken clouds. The method then interprets the scene as a large thin cloud rather than a patchwork of small thick clouds, so that the modeled irradiance varies less and at a lower frequency than what terrestrial instruments would record. Uncertainty in the modeled instantaneous irradiance under intermittent cloudiness is therefore higher than under cloudless or overcast conditions. At low solar elevations, uncertainty in the cloud index generally increases because of complex 3-D reflections effects off the sides of clouds, and parallax effects in the case of high clouds. Additionally, a high surface albedo (e.g., snow-covered areas) lowers the contrast of the signal recorded by the satellite and introduces error in the cloud index. The major challenge here is to correctly attribute any high radiance value retrieved from satellite imagery to either a cloud scene or

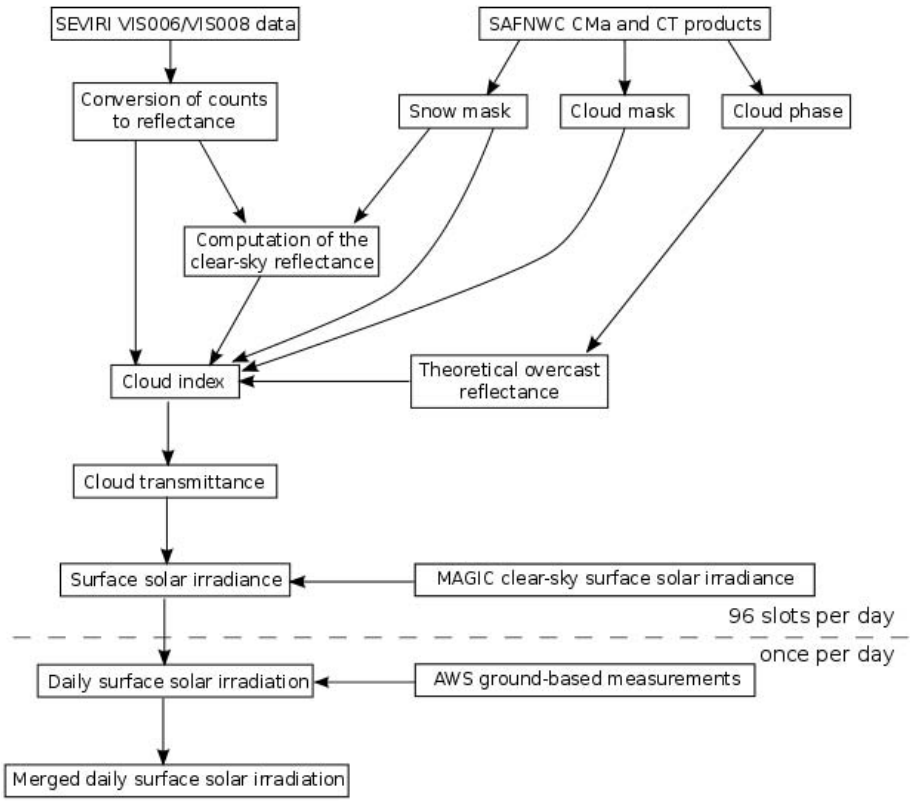

Figure 1. Schematic view of the MAGIC/Heliosat-2 process implemented at RMI.

a high-albedo surface. Uncertainties are thus expected to be higher during winter months.

Measurements from 11 radiometric stations operated by RMI were used to evaluate the performance of our algorithm. Global horizontal irradiance measurements are made with a 5 secondes time step and then integrated on a 10-min basis in the RMI data warehouse where they undergo a set of semi-automatic quality assessment procedures (Journée and Bertrand, 2011). Daily SSI values are obtained by simple summation for the 10-min integrated ground-based measurements and by trapezoidal integration over the diurnal cycle for the MSG-based instantaneous values. The merged daily SSI estimations are obtained using the kriging with external drift geostatistical approach as described in Journée and Bertrand (2010). The retrieved daily all-sky SSI are evaluated first for non-merged data through a direct comparison between satellite derived and ground-measured data and second by leave-one-out cross-validation (CV) for satellite-ground merged estimations on the basis of one year of quality controlled data (i.e., 2011). Two statistical error indices are considered: the mean bias error (MBE) and root mean square error (RMSE).

Table 1 indicates that overall for the year 2011 the satellite-retrieved daily SSI data using climatological input data for the MAGIC clear-sky model (i.e., CLIM(SA,AOD,WVC)) present an overall positive bias of 3.52 % (i.e., a MBE of 119.02 Wh m^{-2}). The bias is maximum in winter and minimum in autumn (i.e., MBE of 7.67 % (67.75 Wh m^{-2}) and of 2.48 % (62.62 Wh m^{-2}) for DJF and SON, respectively). The reported spring and summer biases are in the order of 3.07 % (142.09 Wh m^{-2}) and 3.83 % (167.22 Wh m^{-2}) for MAM and JJA, respectively. The bias originates in the use of RTM simulated overcast visible reflectances, ρ_{max}, in the cloud index, n, computation (see Eq. 1) instead of actual measured overcast reflectances. Simulated overcast visible reflectances tend to overestimate the actual ones (i.e., RTMs provide an upper bound on ρ_{max}, which often exceeds the actual ρ_{max}) which leads to reduce the magnitude of the effective cloud albedo, and subsequently to an increase in the retrieved SSI. While the observation angles of geostationary sensors remain invariable, measurements depend on varying illumination angles and changes during the course of the day/year. The larger bias at wintertime relies on an enhanced overestimation in simulated ρ_{max} at high solar zenith angles (low elevation). Fortunately, correcting the satellite-derived daily SSI values by using in situ measurements reduces the overall model bias to 0.03 % (MBE$_{cv}$ of 1.01 Wh m^{-2}) and its seasonal magnitude (e.g., MBE$_{cv}$ of −0.67 Wh m^{-2} (−0.08 %) for DJF). Finally, thanks to the enhanced SEVIRI scene identification the method does not exhibit a particular weakness over snowed land surface.

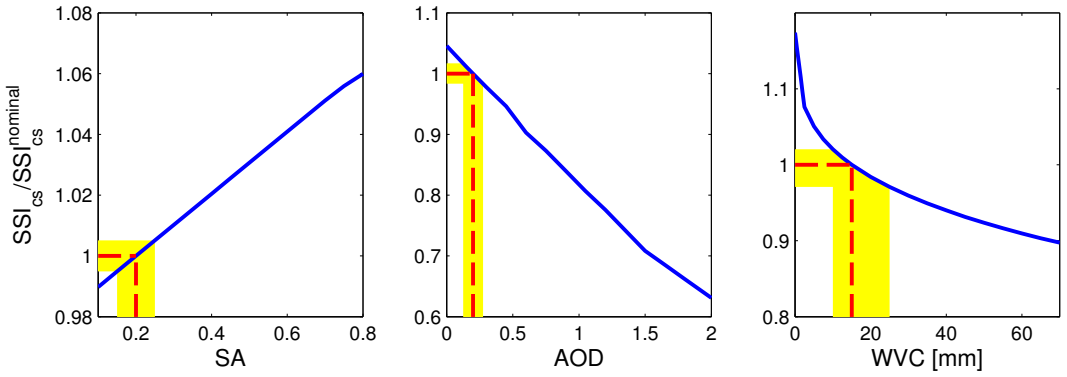

Figure 2. Sensitivity of the MAGIC computed clear-sky SSI with respect to the surface albedo (SA), the aerosol optical depth (AOD) and the atmospheric water vapor content (WVC). Values are normalized with respect to the daily integrated clear-sky SSI computed over Belgium with the nominal values for the 3 parameters (i.e., SA = 0.2, AOD = 0.2 and WVC = 15 mm).

4 Sensitivity of the retrieval scheme to the MAGIC clear-sky model input

To estimate the all-sky irradiance at each time step, the clear-sky SSI is coupled with the cloud index, which acts as a proxy for cloud transmittance. The clear-sky radiative model is at the core of this process, as it calculates solar irradiance for any given sun position, state of the atmosphere, and terrain conditions. The performance of the clear-sky model depends on the physical soundness of its parameterizations, and its ability to deal properly not only with typical cases, but also with extreme values of the main inputs, such as high load of aerosols, extreme humidity conditions, high site elevation, low solar elevation, unusual surface reflectance patterns, or shading effects. The sun geometry is a deterministic parameter, which can be evaluated with satisfactory accuracy. The modeling of how topography affects the direct and diffuse radiation components is also deterministic, but more complex. The site's elevation determines the atmospheric pressure and the related extinction process, whereas the surrounding terrain determines the possible shading of the sun and/or parts of the sky. Accounting for the terrain complicates calculations and requires a spatial resolution at least an order of magnitude better than the nominal resolution of the satellite image (e.g., Cebecauer et al., 2011). Clear-sky atmospheric conditions are variable, both spatially and temporally. These variations are related to the changing concentrations of the main radiatively active atmospheric constituents, namely aerosols, water vapor and ozone. In the current operational scheme, climatological input data are used by the MAGIC clear-sky code. The drawback of such an approach is that long-term averages artificially remove the natural daily fluctuations and the failure to represent extreme events. Moreover, because aerosols and water vapor are highly variable over space and time a relative coarse spatio-temporal resolution of aerosol or water vapor data prevents a detailed rendering of local small-scale patterns and could be a source of bias between estimated and measured SSI.

Figure 2 displays the sensitivity of the MAGIC computed clear-sky SSI with respect to the surface albedo (SA), the aerosol optical depth (AOD) and the atmospheric water vapor content (WVC). Basically, one year of simulations based on a 15-min time step were carried out by running the MAGIC code with SA, AOD, and WVC values covering a large range of variation. In these simulations, each parameter was varied over the largest physical range while the other two were kept fixed to their nominal values for Belgium (annual mean climatological values at Uccle). The results are illustrated in Fig. 2 for the annual mean of the daily integrated clear-sky SSI. Note that values in this figure are normalized with respect to the daily integrated clear-sky SSI computed with the nominal values for the 3 parameters (i.e., SA = 0.2, AOD = 0.2, WVC = 15 mm). Also provided on the panels in Fig. 2 (yellow strip) is the typical variability range for the 3 parameters in Belgium (i.e., SA ranges from 0.15 to 0.25, AOD from 0.125 to 0.275 and WVC from 10 to 25) as retrieved from climatology. Clearly, the largest impact in the simulated MAGIC clear-sky SSI over Belgium is expected to come from the integrated WVC input (variation of ±3.2 % in the simulated annual mean clear-sky daily SSI) and the impact on SSI will be much higher for low atmospheric WVC. By contrast, variation in the simulated annual mean clear-sky daily SSI over Belgium equals ±0.5 % and ±2.1 % for the SA and AOD input values, respectively. Note that for SA values, a large sensitivity up to 5 % could appear in wintertime in the presence of snowed land surface. It is worth pointing out that if a pixel is detected as snowed by the NWC SAF snow mask, a snow albedo is considered in the retrieval process instead of the pixel default albedo value.

To further assess the potential impact of SA, AOD and WVC on the MSG retrieved all-sky daily SSI values, one year (i.e., 2011) of SSI retrievals were performed over the RMI's MAGIC/Heliosat-2 domain by considering for each of the 3 input parameters both the MAGIC default climatological values and time series derived from in situ data, satellite

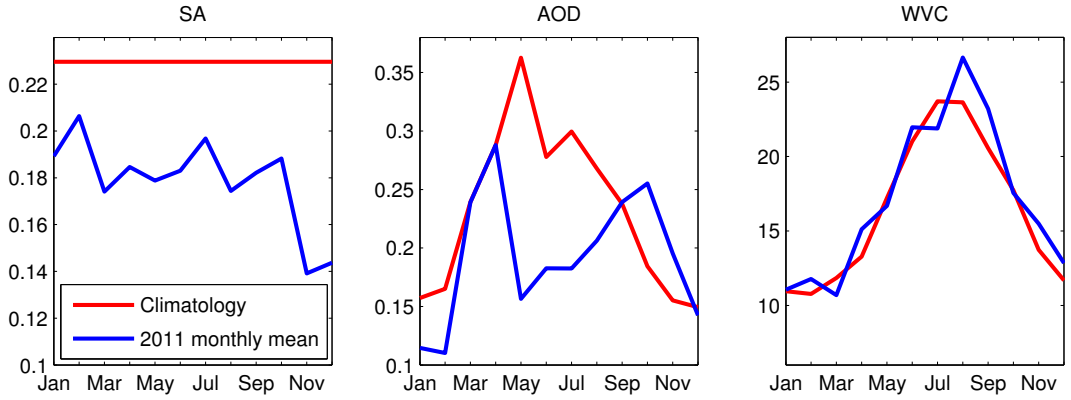

Figure 3. Comparison between climatological and observed/estimated 2011 monthly mean values for surface albedo, aerosol optical depth and water vapor content (in mm) for Uccle (Brussels).

observations or model-based forecasts. Basically, beside the MAGIC default climatological surface albedo data set (i.e., annual mean surface albedo at $1 \times 1°$ spatial resolution from Clouds and the Earth's Radiant Energy System Clouds and Surface and Atmospheric Radiation Budget data product, Rutan and al., 2009) daily surface albedo values produced by the EUMETSAT Land Surface Analysis Satellite Application Facility at the MSG/SEVIRI spatial resolution (Geiger et al., 2008) for the year 2011 were considered. Note that in both cases the MAGIC model accounts for the solar zenith angle dependency of SA. Similarly, a monthly mean AOD data set was generated at the MSG/SEVIRI spatial resolution over Belgium by aggregation of the 10×10 km MODIS Collection 5 aerosols optical depth retrievals over land (Levy et al., 2007) and by combination with AERONET level 2.0 monthly mean AOD values from the 6 AERONET sites located within the domain to supplement the MAGIC AOD default values (i.e., monthly mean AOD at $1 \times 1°$ spatial resolution from Kinne et al., 2006 median model). Finally, 3-hourly water vapor profiles from the $0.25 \times 0.25°$ ECMWF model forecasts updated twice a day and interpolated at each MSG time slot were considered as an additional source of WVC information to the MAGIC WVC default values (i.e., long-term monthly mean values at $0.25 \times 0.25°$ spatial resolution taken from the ECMWF ERA-40/Interim reanalysis data set). Comparison between MAGIC default SA, AOD and WVC values for Uccle (Brussels) and the corresponding 2011 monthly mean estimations is provided in Fig. 3. Note that because ozone has only a small impact on SSI (e.g., Cebecauer et al., 2011), a climatological value is assumed sufficient and no further analysis of the potential impact of this parameter on the retrieval scheme performance was considered here.

Table 1 summarizes in terms of error indices the results obtained for different combinations of the 3 ancillary parameter data sources in the SSI retrieval process against the ground-based measurements. Because SA values from the LSA SAF are lower than the default MAGIC values, use of the LSA SAF albedo product in the retrieval process allows to reduce the overall bias by 1.14 % (e.g., from 119.02 Wh m^{-2} for CLIM(SA,AOD,WVC) to 80.46 Wh m^{-2} for SA+CLIM(AOD,WVC)). While the bias is reduced for each season, the better improvement appears in winter (DJF) where the MBE decreases from 67.75 Wh m^{-2} (7.67 %) for CLIM(SA,AOD,WVC) to 52.49 Wh m^{-2} (or 5.94 %) for SA+CLIM(AOD,WVC). Because the estimated 2011 monthly mean AOD values are lower than the MAGIC default values excepted in autumn (see upper right panel in Fig. 3), use of the 2011 AOD values degrades the overall performance of the method (i.e., MBE of 159.69 Wh m^{-2} and RMSE of 320.53 Wh m^{-2} for the AOD+CLIM(SA+WVC) retrievals vs. MBE of 119.02 Wh m^{-2} and RMSE of 291.05 Wh m^{-2} for the CLIM(SA,AOD,WVC) retrievals, respectively). The largest score reduction occurs at summertime where the MBE for JJA reaches up to 234.19 Wh m^{-2} (or 5.35 %) vs. a MBE of 167.22 Wh m^{-2} or 3.84 % for CLIM(SA,AOD,WVC). Note that on the contrary a slight improvement (RMS reduction of 0.01 %) is reported for SON. Regarding the WVC, because estimations from the ECMWF model forecasts are lower than the MAGIC default values, use of the ECMWF model forecasts tend to increase the overall statistical error indices as indicated in Table 1. However, the situation differing from one season to another, combining both the LSA SAF albedo values and the WVC values from the ECMWF model forecasts in the retrieval process (i.e., SA+WVC+CLIM(AOD) in Table 1) produces the best score in terms of RMSE reduction (273.72 Wh m^{-2} or 8.08 % vs. 291.05 Wh m^{-2} or 8.60 % for CLIM(SA,AOD,WVC)). By contrast, accounting for the WVC values from the ECMWF model forecast and the estimated 2011 monthly mean AOD values generate the worst SSI retrieval in terms of error indices with an overall RMS of 178.99 Wh m^{-2} and a RMSE of 326.93 Wh m^{-2}. Finally, the various statistics provided in Table 1 indicate that the largest improvement in the estimated daily all-sky SSI values over Belgium in terms of bias reduction and RMSE decrease

Table 1. MBE and RMSE of (A) non-merged and (B) merged daily-integrated SSI using the MAGIC default climatology and dynamical inputs (i.e., SA, AOD and WVC) versus global solar radiation measurements at 11 stations in Belgium for the year of 2011.

(A) Non-merged daily integrated SSI				
MAGIC input	MBE ($Wh\,m^{-2}$)	relative MBE (%)	RMSE ($Wh\,m^{-2}$)	relative RMSE (%)
CLIM(SA,AOD,WVC)	119.02	3.52	291.05	8.60
SA+CLIM(AOD,WVC)	80.46	2.38	276.99	8.18
AOD+CLIM(SA,WVC)	159.69	4.72	320.53	9.47
WVC+CLIM(SA,AOD)	138.32	4.09	292.56	8.64
SA+WVC+CLIM(AOD)	99.50	2.94	273.72	8.08
SA+AOD+CLIM(WVC)	120.75	3.57	300.40	8.88
AOD+WVC+CLIM(SA)	178.99	5.29	326.93	9.66
SA+WVC+AOD	139.79	4.13	302.54	8.94
(B) Merged daily integrated SSI				
MAGIC input	MBE_{cv} ($Wh\,m^{-2}$)	relative MBE_{cv} (%)	$RMSE_{cv}$ ($Wh\,m^{-2}$)	relative $RMSE_{cv}$ (%)
CLIM(SA,AOD,WVC)	1.01	0.03 %	244.41	7.22 %
SA+CLIM(AOD,WVC)	−0.06	< 0.01 %	247.71	7.32 %
AOD+CLIM(SA,WVC)	1.74	0.05 %	244.45	7.22 %
WVC+CLIM(SA,AOD)	1.42	0.04 %	243.20	7.19 %
SA+WVC+CLIM(AOD)	0.21	0.01 %	246.60	7.29 %
SA+AOD+CLIM(WVC)	0.74	0.02 %	247.66	7.32 %
AOD+WVC+CLIM(SA)	2.08	0.06 %	243.43	7.19 %
SA+WVC+AOD	0.98	0.03%	246.58	7.29%

is obtained by merging both satellite retrievals and ground-based measurements. Influence of the MAGIC input data sources appears as quite negligible in the merged daily all-sky SSI products. As an example, the reported $RMSE_{cv}$ values in Table 1 differ by less than 5 $Wh\,m^{-2}$ or 0.13 % between the 8 different merged daily products.

5 Conclusions

This study aimed at assessing the sensitivity of the MAGIC/Heliosat-2 method over Belgium to the surface albedo, atmospheric aerosol optical depth and integrated water vapor content values required as input data by the MAGIC clear-sky model. Our results indicate that irrespective of the ancillary data sources for these 3 parameters, our retrieval scheme is positively biased over Belgium. Because simulated overcast visible reflectances tend to overestimate the actual ones our cloud index computation leads to reduce the magnitude of the effective cloud albedo, and subsequently to an increase in the retrieved SSI. Use of observed/estimated values during the retrieval process instead of climatological means can help to reduce to some extent the bias and RMS error between satellite retrieved and ground measured all-sky SSI. The largest errors reduction is obtained when considering both the actual surface albedo and integrated water vapor content values in the retrieval process. Because the estimated 2011 aerosol optical depth values were on average larger than the default MAGIC values, the overall bias of the method was increased when performing the SSI retrievals with these estimations. However, due to limitations in the AOD retrieval process over land surface (e.g., Hsu et al., 2004) and the limited number of AOD measurements available over the domain, it is likely that our estimated 2011 AOD monthly mean time series are only a crude estimation of the actual 2011 AOD values over Belgium. As an example, the summer AOD background value over Belgium appears well underestimated in our reconstruction which therefore tends to reinforce the positive bias of our retrieval scheme compared to the ground observations and subsequently to a worse performance of the model. Finally, whatever the sources of the MAGIC input data may be, the most accurate mapping of the daily all-sky SSI over Belgium is obtained once ground measurements and satellite-based estimation are merged into a single product. Correcting the satellite-derived data by using in situ measurements reduces the overall model bias. Therefore, the influence of the MAGIC input data sources is largely masked in the merged daily integrated all-sky SSI product,

which subsequently appears to be nearly independent of the MAGIC input data sources used during the SSI satellite retrieval process.

Acknowledgements. The authors are grateful to Richard Mueller (German Meteorological Service, Germany) for providing us the MAGIC clear-sky model. We are also grateful to the all of the investigators and their staff who participate in the AErosol RObotic NETwork for establishing and maintaining the sites used in this investigation. This work was supported by the Belgian Science Policy Office (BELSPO) through the ESA/PRODEX program PRODEX-9 contract No. 4000102777 "Surface Solar Radiation".

Edited by: G.-J. Steeneveld
Reviewed by: E. L. A. Wolters, J. Polo, and one anonymous referee

References

Asner, G. P.: Biophysical and Biochemical Sources of variability in Canopy Reflectance, Remote Sens. Environ., 64, 234–253, 1998.

Cano, D., Monget, J. M., Albuisson, M., Guillar, H., Regas, N., and Wald, L.: A method for the determination of the global solar radiation from meteorological satellite data, Sol. Energy, 56, 207–212, 1986.

Cebecauer, T., Suri, M., and Gueymard, C.: Uncertainty sources in satellite-derived direct normal irradiance: how can prediction accuracy be improved globally?, Proceedings of the SolarPACES Conference, Granada, Spain, 20–23 September 2011.

Derrien, M. and Le Gléau, H.: MSG/SEVIRI cloud mask and type from SAFNWC, Int. J. Remote Sens., 26, 4707–4732, 2005.

Geiger, B., Carrer, D., Franchistéguy, L., Roujean, J.-L., and Meurey, C.: Land surface albedo derived on a daily basis from Meteosat Second Generation observations, IEEE T. Geosci. Remote Sens., 46, 3841–3856, 2008.

Hammer, A., Heinemann, D., Hoyer, C., Kuhlemann, R., Lorenz, E., Müller, R., and Beyer, H.: Solar energy assessment using remote sensing technologies, Remote Sens. Environ., 86, 423–432, 2003.

Hsu, N. C., Tsay, S. C., King, M. D., and Herman, J. R.: Aerosol Properties over Bright Reflecting Source Regions, IEEE T. Geosci. Remote Sens., 42, 557–569, 2004.

Ipe, A., Clerbaux, N., Bertrand, C., Dewitte, S., and Gonzalez, L.: Pixel-scale composite top-of-the-atmosphere clear-sky reflectances for Meteosat-7 visible data, J. Geophys. Res., 108, 148–227, 2003.

Journée, M. and Bertrand, C.: Improving the spatio-temporal distribution of surface solar radiation data by merging ground and satellite measurements, Remote Sens. Environ., 114, 2692–2704, 2010.

Journée, M. and Bertrand, C.: Quality control of solar radiation data within the RMIB solar measurements network. Sol. Energy, 85, 72–86, 2011.

Journée, M., Stöckli, R., and Bertrand, C.: Sensitivity to spatio-temporal resolution of satellite-derived daily surface solar irradiation, Remote Sens. Lett., 3, 315–324, 2012.

Kinne, S., Schulz, M., Textor, C., Guibert, S., Balkanski, Y., Bauer, S. E., Berntsen, T., Berglen, T. F., Boucher, O., Chin, M., Collins, W., Dentener, F., Diehl, T., Easter, R., Feichter, J., Fillmore, D., Ghan, S., Ginoux, P., Gong, S., Grini, A., Hendricks, J., Herzog, M., Horowitz, L., Isaksen, I., Iversen, T., Kirkevåg, A., Kloster, S., Koch, D., Kristjansson, J. E., Krol, M., Lauer, A., Lamarque, J. F., Lesins, G., Liu, X., Lohmann, U., Montanaro, V., Myhre, G., Penner, J., Pitari, G., Reddy, S., Seland, O., Stier, P., Takemura, T., and Tie, X.: An AeroCom initial assessment – optical properties in aerosol component modules of global models, Atmos. Chem. Phys., 6, 1815–1834, doi:10.5194/acp-6-1815-2006, 2006.

Lefèvre, M., Diabaté, L., and Wald, L.: Using reduced data sets ISCCP-B2 from the Meteosat satellites to assess surface solar irradiance, Sol. Energy, 81, 240–253, 2007.

Levy, R. C., Remer, L. A., Mattoo, S., Vermote, E. F., and Kaufman, Y. J.: Second-generation operational algorithm: Retrieval of aerosol properties over land from inversion of Moderate Resolution Imaging Spectroradiometer spectral reflectance, J. Geophys. Res., 112, 13211–13221, 2007.

Moradi, I., Müller, R., Alijani, B., and Kamali, G.A.: Evaluation of the Heliosat-II method using daily irradiation data for four stations in Iran, Sol. Energy, 83, 150–156, 2009.

Mayer, B. and Kylling, A.: Technical note: The libRadtran software package for radiative transfer calculations – description and examples of use, Atmos. Chem. Phys., 5, 1855–1877, doi:10.5194/acp-5-1855-2005, 2005.

Müller, R., Dagestad, K-F., Ineichen, P., Schroedter Homscheidt, M., Cros, S., Dumortier, D., Kuhlemann, R., Olseth, J., Piernavieja, G., Reise, Ch., Wald, L., and Heinnemann, D.: Rethinking satellite based solar irradiance modelling – The SOLIS clear sky module, Remote Sens. Environ., 91, 160–174, 2004.

Müller, R., Matsoukas, C., Gratzki, A., Behr, H. D., and Hollmann, R.: The CM-SAF operational scheme for the satellite based retrieval of solar surface irradiance – a LUT based eigenvector hybrid approach, Remote Sens. Environ., 113, 1012–1024, 2009.

Posselt, R., Müller, R., Stöckli, R., and Trentmann, J.: Spatial and temporal Homogeneity of Solar surface Irradiance across satellite generations, Remote Sens., 3, 1029–1046, 2011.

Raschke, E., Gratzki, A., and Rieland, M.: Estimates of global radiation at the ground from reduced data sets of International Satellite Cloud Climatology Project, J. Climate, 7, 205–213, 1987.

Rigollier, C., Lefèvre, M., and Wald, L.: The method Heliosat-2 for deriving shortwave solar radiation from satellite images, Sol. Energy, 77, 159–169, 2004.

Rutan, D., Rose, F., Roman, M., Manalo-Smith, N., Schaaf, C., and Charlock, T.: Development and assessment of broadband surface albedo from Couds and Earth's Radiant Energy System Clouds and Radiation Swath data product, J. Geophys. Res., 114, D08125, doi:10.1029/2008JD010669, 2009.

Schmetz, J., Pili, P., Tjemkes, S., Just, D., Kerkmann, J., Rota, S., and Ratier, A.: An Introduction to Meteosat Second Generation (MSG), B. Am. Meteorol. Soc., 83, 977–992, 2002.